journal

J. Am. Ceram. Soc., 88 [1] 160–167 (2005)
DOI: 10.1111/j.1551-2916.2004.00031.x

Energy Crossovers in Nanocrystalline Zirconia

Michael W. Pitcher,[†] Sergey V. Ushakov, and Alexandra Navrotsky[‡]

Thermochemistry Facility and NEAT ORU, University of California at Davis, California 95616

Brian F. Woodfield, Guangshe Li, and Juliana Boerio-Goates

Department of Chemistry and Biochemistry, Brigham Young University, Provo, Utah 84602

Brian M. Tissue

Department of Chemistry, Virginia Polytechnic Institute and State University, Blacksburg, Virginia 24061

The synthesis of nanocrystalline powders of zirconia often produces the tetragonal phase, which for coarse-grained powders is stable only at high temperatures and transforms into the monoclinic form on cooling. This stability reversal has been suggested to be due to differences in the surface energies of the monoclinic and tetragonal polymorphs. In the present study, we have used high-temperature oxide melt solution calorimetry to test this hypothesis directly. We measured the excess enthalpies of nanocrystalline tetragonal, monoclinic, and amorphous zirconia. Monoclinic ZrO_2 was found to have the largest surface enthalpy and amorphous zirconia the smallest. Stability crossovers with increasing surface area between monoclinic, tetragonal, and amorphous zirconia were confirmed. The surface enthalpy of amorphous zirconia was estimated to be 0.5 J/m^2. The linear fit of excess enthalpies for nanocrystalline zirconia, as a function of area from nitrogen adsorption (BET) gave apparent surface enthalpies of 6.4 and 2.1 J/m^2, for the monoclinic and tetragonal polymorphs, respectively. Due to aggregation, the surface areas calculated from crystallite size are larger than those measured by BET. The fit of enthalpy versus calculated total interface/surface area gave surface enthalpies of 4.2 J/m^2 for the monoclinic form and 0.9 J/m^2 for the tetragonal polymorph. From solution calorimetry, the enthalpy of the monoclinic to tetragonal phase transition for ZrO_2 was estimated to be 10 ± 1 kJ/mol and amorphization enthalpy to be 34 ± 2 kJ/mol.

I. Introduction

Zirconia (ZrO_2) has attracted considerable attention over the last two decades because of its important applications. Besides being used as a ceramic and refractory material, it has also found use as a catalyst,[1] in oxygen sensors,[2] and in fuel cells[3] and is being considered as a gate dielectric.[4] Zirconia exists in three distinct polymorphs. The room-temperature stable form is monoclinic (m), which undergoes reversible phase transformations, to the tetragonal (t) form near 1170°C and the cubic (c) phase near 2370°C. However, syntheses of fine-grained powders of zirconia by precipitation from aqueous solution (and other methods) often yields the tetragonal polymorph.[5]

Several explanations have been proposed for this occurrence of tetragonal zirconia: differences in surface energy between the polymorphs,[5–8] the influence of anionic impurities, the influence of lattice strain, structural similarities between the precursor materials and tetragonal zirconia, and the influence of lattice defects and/or water vapor.[9] There has been debate as to which mechanism is dominant in the stabilization of nanoscale tetragonal zirconia. Recent elegant experiments by Wu *et al.*[10] give strong evidence that nanocrystalline tetragonal zirconia is not just kinetically metastable but can be truly thermodynamically more stable than monoclinic zirconia in air below 1200°C as long as coarsening is precluded.

Reversal in phase stability at the nanoscale has been seen in other oxides, most notably Al_2O_3 and TiO_2. In previous studies using high temperature oxide melt calorimetry for nanocrystalline alumina[11,12] and titania,[13] it was shown that direct measurement of the enthalpy difference between the nanocrystalline polymorphs can separate the contributions of the surface energy and of the enthalpy of phase transition. The goal of the present work is to gather calorimetric evidence concerning the phase stability reversal seen in nanocrystalline zirconia.

II. Experimental Procedure

(1) Synthesis

Phase-pure samples of the amorphous, tetragonal, and monoclinic forms of zirconia were synthesized by modifying a procedure developed by Ciuparu *et al.*[14] A 10% wt/v aqueous solution ($\sim 0.43M$) of zirconyl nitrate ($ZrO(NO_3)_2$) was added dropwise to a 150% excess of hydrazine hydrate ($NH_2NH_2 \cdot H_2O$) at 100°C with stirring. The pH was monitored to ensure that it was greater than 8.5. The milky white suspension was digested at 100°C for 6 days. The precipitate was then washed and centrifuged until the supernatant was neutral and free of nitrate ion. The white powder was dried overnight at 120°C and then calcined at 550°C for 6 h to give amorphous zirconia. Further calcination produced tetragonal and monoclinic zirconia samples of varying crystallite size and surface area (see Table I). Bulk monoclinic zirconia (Alfa-Aesar, Ward Hill, MA, Puratronic®, 99.978% (metals basis)) was dried at 1200°C (Table I).

Table I shows that high surface area nanocrystalline monoclinic zirconia has not been synthesized using the method above. Upon conversion to the monoclinic phase the surface area drops off rapidly. This effect has also been reported by Chuah *et al.*[15] Attempts at producing high surface area phase pure monoclinic nanocrystals using a two-step sintering method,[16] hydrothermal synthesis,[17] and laser vaporization[18] were also unrewarding.

Several mixed monoclinic/tetragonal samples with high surface area were prepared by modifying a hydrothermal synthesis

---

I-Wei Chen—contributing editor

Manuscript No. 10617. Received October 22, 2003; approved July 26, 2004.

Supported by the National Science Foundation, Grant number EAR-123998; NIRT: Surface Reactivity of Nanocrystalline Oxides and Oxyhydroxides. One of the authors (S. V. U.) acknowledges financial support from Motorola and the University of California through the UC-Discovery Grant program. High-resolution TEM imaging was performed at the National Center for Electron Microscopy, Lawrence Berkeley National Laboratory.

[†] Current address: Department of Chemistry, Shasta College, 11555 Old Oregon Trail, Redding, P.O. Box 496006, California 96049-6006.

[‡] Author to whom correspondence should be addressed. e-mail: anavrotsky@uc.davis.edu

Table I. Sample Characterization and Thermochemical Data of Phase Pure Zirconia Samples

Sample ID	Calcination T (°C)†	Phase	H_2O (wt%)	Crystallite size XRD (nm)	XRD‡ SA (m^2/g)	Surface area measured by BET		ΔH_{ds} (J/g)	ΔH_{ds} (kJ/mol)§	ΔH (wrt coarse mon.) (kJ/mol)¶
						m^2/g	m^2/mol			
Aesar	1200	Mon.	<0.0001	45.5	23	1.5	185	581.7±2.4(6)	71.68±0.29(6)	—
036F	1200	Mon.	1.4829	39.0	26	4.0	493	615.0±4.4(6)	69.81±0.54(6)	1.87±0.61
008F	1200	Mon.	1.8729	18.0	57	5.5	678	572±16(6)	62.8±2.0(6)	8.90±2.0
008E	1100	Mon.	0.6350	10.6	97	5.6	690	537±10(6)	63.6±1.3(6)	8.1±1.3
036E	1100	Mon.	1.8348	16.3	63	8.5	1047	544.9±7.8(6)	59.58±0.96(6)	12.1±1.0
008D	1000	Tetr.	<0.0001	16.1	62	5.7	702	499.4±5.7(6)	61.53±0.70(6)	10.15±0.76
036D	1000	Tetr.	3.1678	9.0	112	38.0	4682	471.4±5.2(6)	44.55±0.64(6)	27.13±0.70
008C	875	Tetr.	1.6329	4.9	206	48.5	5976	463.7±6.4(6)	50.25±0.79(6)	21.43±0.84
008B	750	Tetr.	3.1355	5.1	198	74.8	9217	470.8±5.2(6)	44.62±0.65(6)	27.06±0.71
036C	875	Tetr.	2.7035	5.1	198	104.4	12 864	400.3±3.7(6)	37.58±0.46(6)	34.10±0.54
036B	750	Tetr.	2.5347	4.4	230	132.2	16 290	287.7±4.5(6)	24.10±0.56(6)	47.58±0.63

[†] Calcination time was 6 h at 750°–1100°C and 2 h at 1200°C. [‡] Calculated from crystallite size assuming spherical particle shape ($S = 6 \times 10^3/D\rho$ where S is the surface area in m^2/g, D is the diameter of a spherical particle in nm, and ρ is the density in g/cm^3, taken as 5.82 m-ZrO_2, and 5.94 for t-ZrO_2). [§] Corrected for water. Value is the mean of the number of experiments given in parentheses. Error is two standard deviations of the mean. One extra decimal place is retained to avoid extra errors. [¶] For reaction ZrO_2 (monoclinic, coarse)$\rightarrow$$ZrO_2$ (polymorph, nano).

BET, Brunauer–Emmett–Teller.

developed by Yoshimura and Sōmiya.[17] Amorphous hydrous zirconia was precipitated from zirconium (IV) chloride solution with ammonium hydroxide (NH_4OH). It was then washed and centrifuged until the supernatant tested free of chloride and was neutral. Drying at 120°C for 48 h was then carried out. Approximately 0.5 g of the dried powder was then placed in a 23-mL Parr pressure vessel and filled with approximately 10 mL of a mineralizer solution (8% w/v aqueous potassium fluoride (KF)). The vessel was then placed in an oven at 200°C for 24 h. On cooling, the precipitate was washed and centrifuged until the supernatant tested free of fluoride. It was then dried overnight at 100°C. Some of the mixed monoclinic/tetragonal samples obtained were calcined at 500° or 750°C to produce a set of samples with varying crystallite size and surface area (see Table II).

A final mixed monoclinic/tetragonal zirconia sample with extremely high surface area (see Table II) was prepared using a gas-phase condensation technique.[18] A cw-CO_2 laser operated at 45 W was used to evaporate a zirconia target obtained commercially from Cerac, Inc. (Milwaukee, WI) (purity 99.7%). The apparatus has been described in detail elsewhere.[18] Prior to deposition, the synthesis chamber was evacuated to 2.5 Torr using an oil-free diaphragm pump. The target surface was heated to 2700°C (monitored with an optical pyrometer) for 5 min with an unfocused beam. The chamber was then filled with oxygen to a pressure of 10 Torr. The beam was focused (~2 mm spot size) on the target and the target rotated at ~0.15 rpm throughout vaporization (2 h). A stainless steel plate, located about 50 mm from the target collected the particles. The sample was then transferred to an argon-filled glove box using a glove bag. This sample was extremely hygroscopic.

(2) Characterization Techniques

X-ray diffraction (XRD) patterns were collected using an INEL-CPS120 diffractometer (INEL, France) operated at 30 kV and 30 mA. Collection time was approximately 1 h. The phase percentages and apparent crystallite sizes of the samples were determined by Rietveld refinement/whole profile fitting (WPF) using Jade 6 software.[19] Atomic positions and strain were not refined. The standard deviation of the crystallite size obtained from the refinement was 0.1–1.0 nm. However, because the accuracy of this technique is problematic for crystallite sizes smaller than 10 nm, and since the particles' shape and strain contribution to broadening were not considered, we assign an uncertainty of ±1 nm in the estimated absolute crystallite size, for values reported in Tables I and Table II. Transmission electron microscopy (TEM) observations (e.g. Fig. 2) agreed with this estimate of average particle size.

The specific surface area was measured using the Brunauer–Emmett–Teller (BET) technique with a Gemini 2360 instrument (Micromeritics, Norcross, GA). Water contents were determined by weight loss measurements. Zirconia samples, accurately weighed inside a glove box, were heated overnight at or above 1100°C in air. The products were white, implying negligible oxygen deficiency. The difference between the final weight and initial weight was taken to be water content. Raman spectra of the samples were measured using a Chromex Raman 2000 Spectrometer (Chromex, Billerica, MA). The light source was a diode laser operating at 785 nm. Scattered light at the laser wavelength (Rayleigh line) was suppressed using a long-pass cut-off filter. The excitation light was directed at the sample and the back-scattered Raman radiation was collected. A Tylenol (Acetaminophen) tablet was used for calibrating the Raman shifts. Scanning electron microscopy (SEM) studies were

Table II. Sample Characterization and Thermochemical Data for Mixed Phase (m-/t-) Zirconia Samples

Sample ID	Calcination T (°C)	Mon. phase (wt%)	H_2O (wt%)	Crystallite size XRD (nm)		Surface area measured by (BET)		ΔH_{ds} (J/g)	ΔH_{ds} (kJ/mol)†	ΔH (wrt coarse mon.) (kJ/mol)‡
				m	t	m^2/g	m^2/mol			
082	120	62	5.4606	26.0	18.2	57.1	7036	469±12(16)	33.8±1.5(16)	43.59±1.54
094	120	53	7.3954	23.5	20.1	71.3	8786	517.1±9.5(6)	31.1±1.2(6)	49.68±1.22
094	750	89	5.7724	30.1	26.4	20.4	2514	478±18(4)	33.59±2.3(4)	40.77±2.29
096A	120	53	7.9172	24.5	19.1	60.7	7479	533±8.5(6)	30.8±1.0(6)	52.25±1.09
096B	500	56	6.9056	22.9	18.4	43.0	5298	513±13(6)	33.0±1.6(6)	51.16±1.64
096C	750	92	6.4410	31.3	24.8	20.6	2538	531±13(6)	37.5±1.6(6)	35.67±1.65
099	120	51	7.4042	26.3	20.6	61.1	7529	523±15(6)	31.8±1.8(6)	51.08±1.84
GZ1§	—	54	5.8800	4.8	4.0	175.2	21 588	100±36(2)	−16.3±4.5(2)	112.17±4.51

[†] Corrected for water. [‡] Corrected for tetragonal phase, see text for details. [§] Sample prepared by condensation from vapor, product extremely hygroscopic.

BET, Brunauer–Emmett–Teller.

conducted[¶] using a FEI XL30-SFEG high-resolution SEM (FEI, Hillsboro, OR). TEM was performed on Philips CM12 (Philips, Hillsboro, OR) (LaB_6 filament) and CM200 FEG instruments.

(3) Calorimetry

High-temperature drop solution calorimetry in lead borate solvent was performed in a custom-built Calvet twin microcalorimeter described previously.[20,21] Oxygen gas was flushed through the glassware at ~35 mL/min and bubbled through the solvent at ~5 mL/min. This maintains oxidizing conditions, helps remove water evolved from the sample, and agitates the solvent to aid dissolution. All the samples were handled in an argon-filled glove box (O_2 and H_2O <1 ppm). The samples were pressed into pellets (~5 mg) inside the glove box, weighed, and stored in a glass vial. When a stable calorimeter baseline was obtained, the pellet from the glass vial was dropped into the calorimeter. The total time the pellet was exposed to air was less than 2 s. The resultant heat effect, referred to further as "the drop solution enthalpy," consists of the heat content of the sample from room temperature to the calorimeter temperature, the heat of sample dehydration, and the heat of solution. Calorimeter calibration was performed using the heat content of corundum pellets of similar weight.

Thermogravimetric measurements were made with a Netzsch 449 apparatus (Netzsch, Selb, Germany). Samples were heated from room temperature to 1000°C under an argon flow (40 mL/min) at 10°C/min.

III. Results

(1) Structural Characterization and Surface/Interface Areas Estimation

Rietveld analyses on the powder XRD patterns was performed for all samples. The crystallite sizes were refined for all samples and the amounts of the tetragonal and monoclinic forms in the two-phase mixtures were also determined (see Tables II and III). We detected the presence of trace amounts of the monoclinic phase in some of the tetragonal samples with a larger crystallite size listed in Table I, but the percentage was not quantifiable and any small correction for this effect in calorimetry was neglected.

Initial intensity (I/I_0) analysis of the X-ray powder patterns of the higher surface area tetragonal samples (>40 m^2/g) led us to suspect that we had synthesized the cubic form of zirconia. However, Rietveld refinement suggested that the tetragonal polymorph had been formed. Raman data for one of these samples is in excellent agreement with previous Raman studies on zirconia,[22–24] lending further evidence to our samples being tetragonal rather than cubic. Cubic zirconia is expected to have a single Raman band centered around 490 cm^{-1}, whereas tetragonal zirconia should exhibit six Raman bands, with frequencies at about 148, 263, 325, 472, 608, and 640 cm^{-1}. A Raman spectrum for a sample identified as tetragonal (with no monoclinic detectable) by Rietveld refinement is shown in Fig. 1. It confirms that this sample is indeed tetragonal.

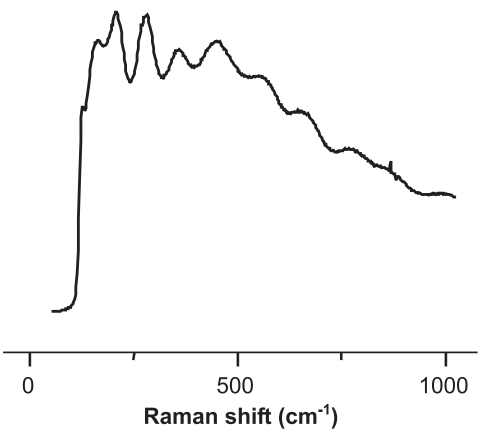

Fig. 1. Raman spectrum of a nanocrystalline sample of tetragonal zirconia (36C in Table I). This sample does not contain any monoclinic phase by X-ray diffraction.

There have been several literature claims for the synthesis of the nanophase cubic zirconia.[25–29] These syntheses employ various strategies including the utilization of the sol–gel reaction and precipitation in the presence of various polymers. Our attempts at repeating these syntheses have yielded only the tetragonal and monoclinic polymorphs, as confirmed by Rietveld refinement of their XRD patterns. We suspect that the material identified as cubic in earlier studies may well have been tetragonal.

Surface areas measured by BET and crystallite size determined from Rietveld refinement of XRD patterns are shown in Tables I and II. The total surface/interface area calculated by assuming single-crystal spherical particles is significantly higher than that accessible for nitrogen adsorption. This indicates significant aggregation in the samples. This is confirmed by SEM and TEM imaging (e.g., Fig. 2).

(2) Calorimetry

Tables I and III list the enthalpies of drop solution. The enthalpy difference between a nanocrystalline sample and bulk monoclinic zirconia arises from polymorphism, surface energy, and the presence of water. The latter has to be accounted for in the thermochemical cycle. For the purposes of the current investigation we used the same assumption as in our previous studies of amorphous zirconia[30,31] and nanocrystalline titania[13] that the water present in all nanocrystalline zirconia samples is energetically equivalent to bulk liquid water. This will be discussed in detail below. Therefore, the excess enthalpy of the nanocrystalline polymorphs (n) with respect to the most stable phase, namely coarse monoclinic zirconia (m), can be calculated using the following thermochemical cycle:

$$ZrO_2\ (n,\ 25°C)\cdot xH_2O\ (l,\ 25°C) \rightarrow (\text{dilute solution},\ 700°C) + xH_2O\ (g,\ 700°C)\uparrow \qquad \Delta H_{ds}\ (n)$$

Table III. Summary of Thermochemical Data for Amorphous Zirconia

Sample ID	Calcination T (°C)	H_2O (wt%)	SA BET, (m^2/mol)	ΔH_{ds} (J/g)	ΔH_{ds} (kJ/mol)	ΔH_{trans} (kJ/mol)[‡‡]	Method, reference
BZ01[†]	140	10.55	1183	$305.3\pm9.5(7)$	-13.6 ± 1.2	33.3 ± 2.2	$3Na_2O\cdot4MoO_3$ at 700°C[‖]
ZS91bc[‡]	600	<0.01	20 000	$354.0\pm6.7(6)$	41.70 ± 0.89	43.0 ± 1.5	$2PbO\cdot B_2O_3$ at 800°C[††]
036A	550	5.0457	30 694	$358.2\pm5.9(6)$	21.40 ± 2.6	50.3 ± 2.6	$2PbO\cdot B_2O_3$ at 700°C
BZM[§]	300	13.0	33 031	$669\pm19(7)$	20.2 ± 2.7	58.6 ± 3.3	$2PbO\cdot B_2O_3$ at 800°C
ZrO_2/An[¶]	—	2–4	42 000	—	-30.4 ± 4.6	50.1 ± 4.9	$3Na_2O\cdot4MoO_3$ at 700°C

[†] Precipitated from $ZrOCl_2\cdot8H_2O$ with NH_4OH. [‡] Sol–gel synthesis with 10 at% SiO_2 quenched in DSC before crystallization, surface area estimated from crystallite size after crystallization. [§] Precipitated from $ZrOCl_2\cdot8H_2O$ with NH_4OH surface area calculated from particle size (3.8 nm) from TEM.[30] [¶] Extrapolated from anatase-amorphous ZrO_2 drop solution calorimetry. [‖] ΔH_{ds} ZrO_2 (coarse, mon. lead borate, 800°C) = $84.69\pm1.17(8)$ kJ/mol; ΔH_{ds} SiO_2 glass in lead borate at 800°C = 38.72 ± 0.75 kJ/mol. [††] ΔH_{ds} ZrO_2 (coarse, mon in sod. moly, 700°C) = $19.7\pm1.8(9)$ kJ/mol.[31] [‡‡] Corrected for water. Value is the mean of the number of experiments indicated in parentheses. Error is 2 SD of the mean.

BET, Brunauer–Emmett–Teller.

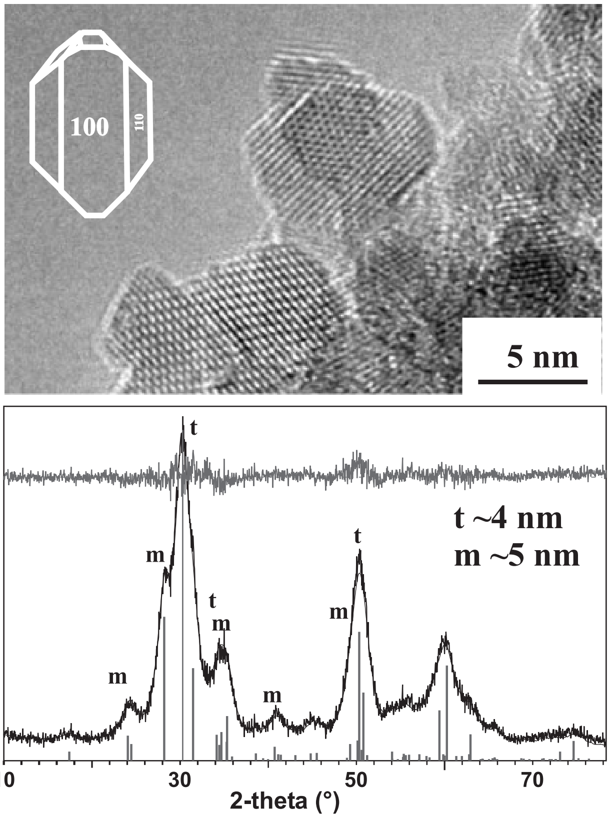

Fig. 2. Sample of nanocrystalline zirconia from laser evaporation (GZ1). Top: high-resolution transmission electron microscopy micrograph, typical crystal habit for naturally occurring monoclinic ZrO_2 (baddelyte) shown on inset. Bottom: XRD pattern and difference for Rietveld fit for the same sample, m, monoclinic; t, tetragonal reflections.

ZrO_2 (m, 25°C)→(dilute solution, 700°C) ΔH_{ds} (m)
H_2O (l, 25°C)→H_2O (g, 700°C) ΔH (water)

The enthalpy for the reaction

$$ZrO_2(m, 25°C) = ZrO_2(n, 25°C)$$

can be obtained as

$$\Delta H(m \rightarrow n) = \Delta H_{ds}(m) - \Delta H_{ds}(n) + \Delta H(\text{water})$$

The excess enthalpy of nanocrystalline polymorphs with respect to coarse monoclinic zirconia can be thought of as the sum of the enthalpy due to polymorphism and that due to increased surface area. The latter is thought of as a surface enthalpy but, as particles get smaller, the distinction between relaxation/restructuring at the surface and in the bulk becomes less clear. The excess enthalpy can be written as follows, using nanophase tetragonal zirconia (n,t) as an example:

$$\Delta H(m \rightarrow n, t) = A_{(t)}\gamma(t) + \Delta H_{trans}(m \rightarrow t)$$

where γ is the surface enthalpy and A is the surface area. We know the surface area of the samples from BET measurements. Thus, by plotting enthalpy versus surface area for the different polymorphs, we can obtain the surface and transition enthalpies. Since we were not able to synthesize pure monoclinic zirconia with BET surface areas larger than 10 m^2/g, the excess enthalpy for nanoscale monoclinic zirconia was derived from the mixed monoclinic/tetragonal zirconia samples, as shown in Table II. The contribution to the excess enthalpy from the tetragonal phase in the samples was calculated using the linear fit for pure tetragonal zirconia (Fig. 3, ΔH (kJ/mol) = $0.0021A+10.61$) and its crystallite size and weight percent as determined by refinement of the XRD data.

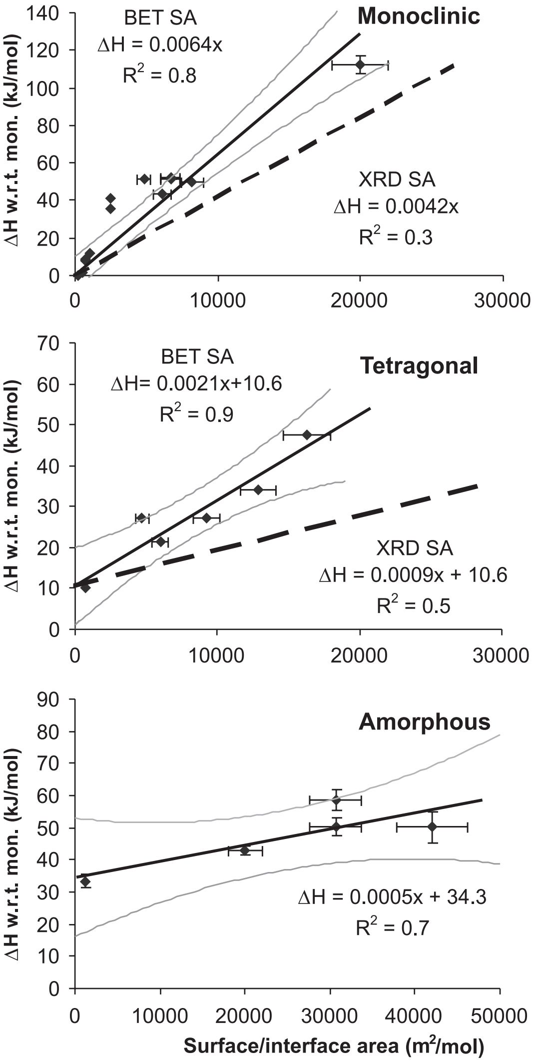

Fig. 3. Enthalpy of nanocrystalline zirconia polymorphs with respect to bulk monoclinic zirconia. Data points shown for BET surface area (SA). Thin lines represent 95% confidence limits for data fit. Dashed lines represent the fit if surface areas calculated from XRD are used and are considered less accurate, see text.

(3) Amorphous Zirconia

Table III presents the calorimetric data for amorphous zirconia from this work and other drop solution experiments conducted in our laboratory.[30,31] Besides pure amorphous zirconia samples synthesized by precipitation, we have included data for high surface area amorphous zirconia obtained from a series of samples supported on TiO_2 (anatase) with varying Zr/Ti ratio,[31] and data from ZrO_2 with 10 mol% SiO_2.[32] All data points form a close to linear trend versus surface area (Fig. 3). This suggests that the difference between the surface energy of the pure hydrated amorphous zirconia and its interface energy in the nanocomposites with anatase and silica is too small to be distinguished in these experiments.

From solution calorimetry data, the surface enthalpy of amorphous zirconia is 0.5 ± 0.1 J/m^2 and the estimated amorphization enthalpy of bulk monoclinic zirconia is 34.3 ± 2.2 kJ/mol. The difference in enthalpy between amorphous and tetragonal zirconia, extrapolated to zero surface area, 22.6 ± 2.2 kJ/mol, is in excellent agreement with the amorphization enthalpy (negative of crystallization enthalpy) measured by differential scanning calorimetry (DSC) for low surface area amorphous zirconia, 22.4 ± 1.2 kJ/mol.[33]

(4) Tetragonal Zirconia

Figure 3 shows the excess enthalpies (relative to the coarse monoclinic phase) of nanocrystalline tetragonal zirconia samples (kJ/mol) versus surface area (m^2/mol) as measured by BET. A linear fit (with 95% confidence envelope) yields both the surface enthalpy (slope) and bulk phase transformation enthalpy (intercept). From the graph, the surface enthalpy is 2.1 ± 0.05 J/m^2 and the transformation enthalpy of bulk monoclinic to bulk tetragonal is 10.61 ± 0.57 kJ/mol.

(5) Monoclinic Zirconia

Figure 3 shows the enthalpy of nanoscale monoclinic samples compared with bulk monoclinic zirconia. For monoclinic zirconia $\Delta H(\mathrm{m} \rightarrow \mathrm{n}) = A\gamma$. A linear fit (with 95% confidence intervals) is therefore forced through the origin. The surface enthalpy obtained for monoclinic zirconia is significantly larger than that for tetragonal. Using BET data for surface area, the surface enthalpy of nanocrystalline monoclinic zirconia is 6.4 ± 0.2 J/m^2. The linear fit for the monoclinic data is not as good as that for the tetragonal polymorph. Several samples with a relatively low BET surface area have higher excess enthalpy than would be expected from the linear trend. These correspond to samples with more than 5 wt% water that were synthesized by refluxing under hydrothermal conditions and dried at 120°C. It is entirely possible that, due to these synthesis conditions, some of the remaining water in these samples may be structural rather than physisorbed. Our water correction does not take this scenario into account.

IV. Discussion

Wilson[34] gave an excellent definition for the process of interpreting calorimetric data: "Calorimeters faithfully record all the changes that occur in a sample. A temptation is to mould the resulting calorimetric signal into a pre-conceived idea, but although getting a result from a calorimeter is easy, to get a correct result takes a lot of time, effort and cogitation." This is especially true when one is dealing with nanophase materials, since the number of variables increases and so increase the spread in the data and error sources. At the same time, characterization techniques are often less accurate or too local. Keeping this in mind, let us first consider what would be the ideal samples for calorimetric measurements of surface energy and then discuss what deviations from ideality we have and how they might affect the interpretation of our data.

Obviously, for measuring the surface energy of zirconia polymorphs, it is necessary to have samples of the different polymorphs with varying surface area. Ideally, every nanoparticle in the powder would be a single crystal with an equilibrium crystal shape and of the same size. The crystal faces of our nanocrystals should be atomically clean, with no adsorbed water or carbonates. In this case, BET measurements would give all the surface area that contributes to excess enthalpy and the differences in surface energies between different crystal planes could be derived from the crystal shape. These ideal conditions can never be realized, though. Our samples contain water and the crystallites not only form aggregates but also are not of equilibrium shape. We discuss these effects below.

(1) Correction for Water and Hydration Enthalpy

We have attributed all weight loss in our samples to the presence of water and assumed a zero adsorption enthalpy relative to liquid water. Reported experimental data on the hydration enthalpy of zirconia are scarce. The formation enthalpy for amorphous $ZrO_2 \cdot 5H_2O$ was reported as −2616.3 kJ/mol in a NBS circular[35] in a table dated 1949. Using formation enthalpies for monoclinic ZrO_2 (−1100.6 kJ/mol)[36] and liquid water, one can calculate the hydration enthalpy to be about –98 kJ per mole of ZrO_2 or approximately −20 kJ per mole of bound water. However, the source for these data has not been found. Latimer[37] casts doubt on this value, pointing to its large difference from the reported hydration enthalpy of TiO_2. Turnbull, when conducting calorimetric studies of the reactions of zirconium halides with an aqueous solutions of sodium hydroxide, reported that the formation enthalpy of hydrous ZrO_2 is less than 5 kJ/mol different from that of monoclinic ZrO_2 and concluded that the water in hydrous ZrO_2 "must be only loosely held by physical trapping in the micelles of the solid."[38] The fact that some water is still found in nanocrystalline zirconia heated to 400°C suggests that not all the water is loosely held. The structural heterogeneity of oxide surfaces supports the observation that the heat of adsorption usually becomes less exothermic with increasing coverage.[39] Since in hydrous zirconia the bulk of the weight loss (observed by thermogravimetry) occurs below 400°C, the "loosely held" water assumption probably is reasonable. Nevertheless, we stress that our data most probably relate to hydroxylated surfaces. No calorimetric studies on atomically clean surfaces have been reported to date.

(2) Aggregation in Powders and Interface Energies

Assuming that the surface area, as measured by BET, is the only source of excess enthalpy relative to a bulk phase of the same structure, our data yield surface energies for monoclinic and tetragonal zirconia polymorphs of 6.4 ± 0.2 and 2.1 ± 0.05 J/m^2, respectively. The errors reported are derived from how well the linear trend fits the experimental data (R^2 value) and from propagated errors in the measured drop solution enthalpy and the BET surface areas for individual samples. However, we know from the crystallite size, as determined by XRD and by TEM imaging, that our samples are aggregated, thus not all the surface is accessible for measurement by BET. This "internal" surface (and/or interface) contribution is neglected when the BET surface area is used for calculations. The total surface/interface area can be estimated from crystallite size measured by XRD, assuming spherical particles. A linear fit of the excess enthalpies versus surface areas, calculated in this way, yields surface enthalpies for the monoclinic and tetragonal polymorphs of 4.2 and 0.9 J/m^2. However, the R^2 of the linear fit using XRD-derived surface areas is much worse than for the fit for BET surface areas (see Fig. 3). This might be due to several factors: (i) the larger errors in surface/interface areas calculated from XRD crystallite size; (ii) specific interfacial energies depend on the degree of interface coherence, thus their values may differ in samples prepared under different conditions; and (iii) our samples have different degrees of aggregation and the contribution of interfacial areas to total surface area is not constant, thus excess enthalpies may not depend linearly on surface areas calculated from XRD crystallite size. We are not able to separate the contribution of interfacial enthalpy to the total excess enthalpy. Additional experiments are needed on samples with the same crystallite size, but with different degrees of aggregation. Such samples are not easy to make. For the present study, considering all sources of error, the quality of fit, and consistency with previous studies on Al_2O_3[11,12] and TiO_2,[13] we consider the surface enthalpies derived from the BET areas as more reliable.

(3) Phase Transition Enthalpies and Stability Crossovers

The monoclinic to tetragonal transformation enthalpy (at 25°C), which we have obtained from extrapolation of the oxide melt calorimetry data, is 10.61 ±0.57 kJ/mol. Our estimate lies between the values of Mitsuhashi *et al.*[7] (12.5 kJ/mol) and Coughlin and King[40] (5.94 kJ/mol). Those studies did not consider surface area or water content as possible variables.

Figure 4 summarizes the enthalpy of nanocrystalline zirconia using the BET surface area. The darker line segments show the phases of lowest enthalpy as a function of surface area. Crossovers in the phase of lowest enthalpy are seen for ZrO_2, as have been seen for $A1_2O_3$ (corundum and spinel)[11,12] and TiO_2 (rutile brookite, and anatase).[13] As in those systems, the more metastable the coarse phase (higher intercept in Fig. 4), the lower its surface enthalpy (slope in Fig. 4). These crossovers suggest that for ZrO_2, as for the Al_2O_3 and TiO_2, polymorphs metastable as coarse phases may become thermodynamically stable at the nanoscale.

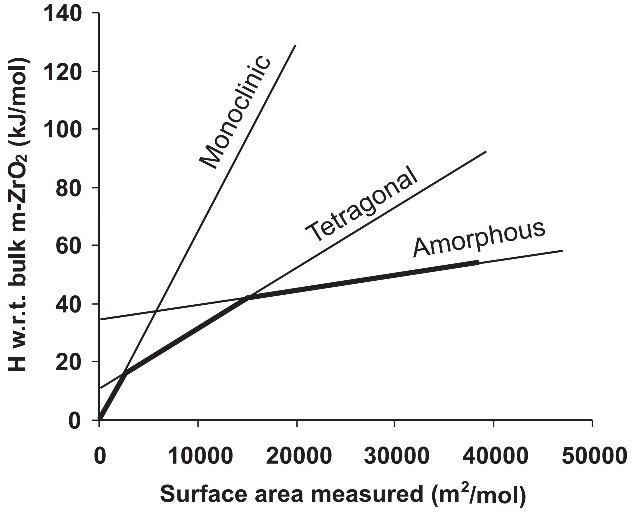

Fig. 4. Phase stability crossover of nanocrystalline zirconia. The darker line segments indicate the energetically stable phases.

(4) Entropy and Gibbs Free Energy of Phases

Phase stability in a thermodynamic sense, of course, is governed by the Gibbs free energy ($\Delta G = \Delta H - T\Delta S$) rather than the enthalpy alone. There are two effects that must be considered. The first is any change in entropy arising from differences in surface area. For CoO nanoparticles, recent measurement of heat capacity by adiabatic calorimetry[40] confirms that the entropy difference between 7-nm nanoparticles and coarse material is small. It is probably reasonable to presume similar behavior for ZrO_2. The second factor is differences in entropy arising from polymorphism. Low-temperature heat capacity and entropy data, measured by adiabatic calorimetry, are available for monoclinic and yttria-stabilized cubic zirconia[41,42] but not for tetragonal zirconia. We can obtain an estimate of the entropy difference between monoclinic and tetragonal zirconia from our value of the phase transformation enthalpy of monoclinic to tetragonal zirconia. Since, for a phase transition, $\Delta G = 0 = \Delta H - T\Delta S$, then substituting $\Delta H = 10.6$ kJ/mol and $T = 1443$ K for the transition, one gets $\Delta S = 7.3$ J $(\mathrm{mol}\cdot\mathrm{K})^{-1}$, i.e., tetragonal zirconia is 7.3 J $(\mathrm{mol}\cdot\mathrm{K})^{-1}$ higher in entropy than monoclinic zirconia. At room temperature this will result in ΔG (of tetragonal zirconia with respect to bulk monoclinic zirconia) being approximately 2 kJ/mol less endothermic than ΔH. Since the tetragonal phase is higher in entropy than the monoclinic, and the amorphous is presumably higher still, the effect of $T\Delta S$ will be to shift the crossovers to somewhat lower surface area (larger particle size).

Whether the monoclinic–tetragonal transition in zirconia at small particle sizes is largely controlled by thermodynamics or by kinetic factors has been disputed for at least 20 years. Garvie[5,6] presented a thermodynamic argument in terms of stability crossovers at the nanoscale that appears to be supported by our calorimetric data. Others[33,43,44] have argued that small tetragonal crystals are metastable and their rate of transformation is controlled by martensitic nucleation kinetics. We note that the situation may be fairly different in relatively dense anhydrous ceramics at high temperature than in hydrated nanoparticles. Our observed crossovers in energetics suggest that, at least for the latter case, a thermodynamic stability field of tetragonal (and amorphous) zirconia at the nanoscale exists. Such materials are, of course, metastable with respect to coarsening and subsequent transformation to the monoclinic phase.

The formation of nanoparticles of a given size and phase distribution from an aqueous solution is almost certainly controlled by the processing route and generally does not represent thermodynamic equilibrium. However, their subsequent coarsening and phase transformation must reflect the observed thermodynamics, inasmuch as phase transformation must occur with a decrease in free energy. Because the rates of grain growth and phase transformation generally follow different kinetic and mechanistic pathways, many transformation scenarios (and distribution of products) can be consistent with the crossovers in enthalpy and free energy.

(5) Previously Reported Values of Surface Enthalpies/ Energies

The literature values for the surface enthalpies of the different polymorphs of zirconia, reported to date, are summarized in Table IV, along with the values obtained in this work. The measurements previously conducted on amorphous zirconia in our laboratory[30–32] are consistent with our new data (Table III). Mitsuhashi *et al.*[7] also used high-temperature oxide melt solution calorimetry to deduce the surface energies of monoclinic and tetragonal zirconia to be 1.2 and 1.1 J/m^2, respectively. They

Table IV. Reported Transformation and Surface Enthalpies for Zirconia Polymorphs

γ (J/m^2)	$\Delta H_{\mathrm{trans}}$ (kJ/mol)†	Method, reference
γ am.	0.7	Approx. from oxide melt calorimetry, Molodetsky *et al.*[30]
	0.5±0.1	Oxide melt calorimetry, this work
γ tetr.	0.59	At 1850°C for Ca-stabilized ZrO_2, based on interfacial angles[46]
	1.9±0.5	Based on critical crystallite size, Molodetsky *et al.*[30]
	1.11	Oxide melt calorimetry, Mitsuhashi *et al.*[7]
	2.1±0.05	This work, using surface area from BET
	~0.9	This work, using total surface/interface area from XRD‡
	1.13	Based on crystallite size effect, Garvie[5]
γ mon.	1.46	Based on crystallite size effect, Garvie[6]
	1.23	Oxide melt calorimetry, Mitsuhashi *et al.*[7]
	6.4±0.2	This work, using surface area from BET
	~4.5	This work, using total surface/interface area from XRD‡
$\Delta H_{\mathrm{trans}}$ (kJ/mol)		
$\Delta H_{\mathrm{trans}}$ m→t	5.94±0.4	Drop calorimetry, Coughlin and King[40]
	12.5	Oxide melt calorimetry, Mitsuhashi *et al.*[7]
	10.61±0.57	Oxide melt calorimetry, this work
$\Delta H_{\mathrm{trans}}$ a→t	−22.4±1.2	At 450°C, differential scanning calorimetry, Ushakov *et al.*[32]
	−22.6±2.2	Oxide melt calorimetry, this work
$\Delta H_{\mathrm{trans}}$ a→m	−34.3±2.2	Oxide melt calorimetry, this work

†Transformation ($\Delta H_{\mathrm{trans}}$) and surface ($\gamma$) enthalpies values are given for room temperature, unless otherwise noted. ‡Considered less accurate than from BET. BET, Brunauer–Emmett–Teller; XRD, X-ray diffraction.

reported the monoclinic to tetragonal transition enthalpy as 12.5 kJ/mol. We believe that this discrepancy may arise because they did not apply any correction for the water content in nanophase zirconia, which is probably substantial for their samples from hydrothermal synthesis.

Garvie[5,6] first suggested in 1965 that stabilization of tetragonal zirconia in fine-grained powders is due to its lower surface energy compared with monoclinic zirconia. By using a critical particle size of 30 nm (from XRD), a value of 0.77 J/m^2 for the surface energy for tetragonal zirconia and a value of 5.94 kJ/mol for the monoclinic to tetragonal transition enthalpy, Garvie calculated the surface energy of monoclinic zirconia as 1.13 J/m^2. If we use data from our work, namely a monoclinic to tetragonal transition enthalpy of $\sim$10 kJ/mol and a surface enthalpy of tetragonal zirconia of $\sim$2 J/m^2, then to get a crossover from tetragonal to monoclinic zirconia at a particle size of 30 nm requires the surface energy of monoclinic zirconia to be approximately 4.5 J/m^2. This is reasonably close to the value we measured. Molodetsky *et al.*[30] observed the critical size for the amorphous to tetragonal transition at 3.5 nm and calculated the surface energy for the tetragonal phase as 1.9 J/m^2, which is in very good agreement with the data in this study.

Recently, the surfaces of zirconia polymorphs were studied by first-principles calculations using density functional theory and the pseudopotential formalism.[45] They concluded that the surface energy of the most stable monoclinic (-111) and tetragonal (111) relaxed surfaces are equal within the calculational accuracy (1.246 vs 1.239 J/m^2 at $T = 0$ K) and proposed that surface energy anisotropy is the key for understanding the stabilization of tetragonal zirconia in nanocrystals. This emphasizes the importance of experimentally established benchmarks in the energetics of zirconia surfaces.

V. Summary and Conclusions

By high-temperature oxide melt solution calorimetry we have measured the excess enthalpies in the monoclinic, tetragonal, and amorphous zirconia polymorphs of varying surface area. This yields a stability map for nanocrystalline and amorphous zirconia and gives an independent estimate of phase transition and amorphization enthalpies in bulk phases. All nanocrystalline phases are thermodynamically metastable with respect to coarse monoclinic zirconia but with increasing surface/interface area, monoclinic zirconia gains excess enthalpy faster than tetragonal zirconia. Amorphous zirconia has the lowest surface energy and becomes energetically favorable over crystalline phases at high surface areas.

Acknowledgments

We thank Juraj Majzlan, John M. Neil, and Hongwu Xu for assistance and discussion and William H. Casey for use of the BET apparatus.

References

[1] X. Song and A. Sayari, "Sulfated Zirconia-based Strong Solid-Acid Catalysts: Recent Progress," *Catal. Rev. Sci. Eng.*, **38** [3] 329–412 (1996).

[2] J. W. Schwank and M. DiBattista, "Oxygen Sensors: Materials and Applications," *MRS Bull.*, **24** [6] 44–8 (1999).

[3] S. Park, J. M. Vohs, and R. J. Gorte, "Direct Oxidation of Hydrocarbons in a Solid-Oxide Fuel Cell," *Nature*, **404**, 265–7 (2000).

[4] A. A. Demkov, "Investigating Alternative Gate Dielectrics: A Theoretical Approach," *Phys. Stat. Sol. (b)*, **226** [1] 57–67 (2001).

[5] R. C. Garvie, "The Occurrence of Metastable Tetragonal Zirconia as a Crystallite Size Effect," *J. Phys. Chem.*, **69**, 1238–43 (1965).

[6] R. C. Garvie, "Stabilization of the Tetragonal Structure in Zirconia Microcrystals," *J. Phys. Chem.*, **82** [2] 218–24 (1978).

[7] T. Mitsuhashi, T. Ikegami, A. Watanabe, and S. Matsuda, "Thermodynamics of Zirconia System with a Possibility of Intelligent Characters," *Proc. Int. Conf. Intell. Mater.*, **1**, 155–8 (1992).

[8] A. Suresh, M. J. Mayo, W. D. Porter, and C. J. Rawn, "Crystallite and Grain-Size-dependent Phase Transformations in Yttria-Doped Zirconia," *J Am. Ceram. Soc.*, **86** [2] 360–2 (2003).

[9] G. Štefanić and S. Musić, "Factors Influencing the Stability of Low Temperature Tetragonal ZrO_2," *Croat. Chem. Acta*, **75** [3] 727–67 (2002).

[10] N. -L. Wu, T. -F. Wu, and I. A. Rusakova, "Thermodynamic Stability of Tetragonal Zirconia Nanocrystallites," *J. Mater. Res.*, **16** [3] 666–9 (2001).

[11] J. M. McHale, A. Auroux, A. J. Perrota, and A. Navrotsky, "Surface Energies and Thermodynamic Phase Stability in Nanocrystalline Aluminas," *Science*, **277**, 788–91 (1997).

[12] J. M. McHale, A. Navrotsky, and A. J. Perrota, "Effects of Increased Surface Area and Chemisorbed H_2O on the Relative Stability of Nanocrystalline γ-Al_2O_3 and α-Al_2O_3," *J. Phys. Chem. B.*, **101**, 603–13 (1997).

[13] M. R. Ranade, A. Navrotsky, H. Z. Zhang, J. F. Banfield, S. H. Elder, A. Zaban, P. H. Borse, S. K. Kulkarni, G. S. Doran, and H. J. Whitfield, "Energetics of Nanocrystalline TiO_2," *Proc. Natl. Acad. Sci.*, **99** [Suppl. 2] 6476–81 (2002).

[14] D. Ciuparu, A. Ensuque, G. Shafeev, and F. Bozon-Verduraz, "Synthesis and Apparent Bandgap of Nanophase Zirconia," *J. Mater. Sci. Lett.*, **19**, 931–3 (2000).

[15] G. K. Chuah, S. Jaenicke, S. A. Cheong, and K. S. Chan, "The Influence of Preparation Conditions on the Surface Area of Zirconia," *Appl. Catal. A: Gen.*, **145**, 267–84 (1996).

[16] I. -W. Chen and X. -H. Wang, "Sintering Dense Nanocrystalline Ceramics Without Final-stage Grain Growth," *Nature*, **404**, 168–71 (2000).

[17] M. Yoshimura and S. Sōmiya, "Hydrothermal Synthesis of Crystallized nanoparticles of Rare Earth-doped Zirconia and Hafnia," *Mater. Chem. Phys.*, **61**, 1–8 (1999).

[18] H. Eilers and B. M. Tissue, "Synthesis of Nanophase ZnO, Eu_2O_3 and ZrO_2 by Gas-phase Condensation with CW-CO_2 Laser Heating," *Mater. Lett.*, **24**, 261–5 (1995).

[19] JADE, Materials Data Inc., Livermore, CA (2002).

[20] A. Navrotsky, "Progress and New Directions in High Temperature Calorimetry Revisited," *Phys. Chem. Min.*, **2**, 89–104 (1977).

[21] A. Navrotsky, "Progress and New Directions in High Temperature Calorimetry," *Phys. Chem. Min.*, **24**, 222–41 (1997).

[22] D. Simeone, J. L. Bechade, D. Gosset, A. Chevarier, P. Daniel, H. Pilliaire, and G. Baldinozzi, "Investigation on the Zirconia Phase Transition Under Irradiation," *J. Nucl. Mater.*, **281**, 171–81 (2000).

[23] A. A. M. Ali and M. I. Zaki, "HT-XRD, IR and Raman Characterization of Metastable Phases Emerging in the Thermal Genesis Course of Monoclinic Zirconia Via Amorphous Zirconium Hydroxide: Impacts of Sulfate and Phosphate Additives," *Thermochim. Acta*, **387**, 29–38 (2002).

[24] P. E. Quintard, P. Barbéris, A. P. Mirgorodsky, and T. Merle-Méjean, "Comparative Lattice-Dynamical Study of the Raman Spectra of Monoclinic and Tetragonal Phases of Zirconia and Hafnia," *J. Am. Ceram. Soc.*, **85** [7] 1745–9 (2002).

[25] J. Zhao, W. Fan, D. Wu, and Y. Sun, "Stable Nanocrystalline Zirconia Sols Prepared by a Novel Method: Alcohol Thermal Synthesis," *J. Mater. Res.*, **15** [2] 402–6 (2000).

[26] A. Chatterjee, S. K. Pradhan, A. Datta, M. De, and D. Chakavortky, "Stability of Cubic Phase in Nanocrystalline ZrO_2," *J. Mater. Res.*, **9** [2] 263–5 (1994).

[27] J. C. Ray, R. K. Pati, and P. Pramanik, "Chemical Synthesis and Structural Characterization of Nanocrystalline Powders of Pure Zirconia and Yttria Stabilized Zirconia," *J. Eur. Ceram. Soc.*, **20**, 1289–95 (2000).

[28] S. Roy and J. Ghose, "Synthesis of Stable Nanocrystalline Cubic Zirconia," *Mater. Res. Bull.*, **35**, 1195–203 (2000).

[29] M. L. Rojas-Cervantes, R. M. Martin-Aranda, A. J. Lopez-Peinado, J. De, and D. Lopez-Gonzalez, "ZrO_2 Obtained by the Sol–Gel Method: Influence of Synthesis Parameters on Physical and Structural Characteristics," *J. Mater. Sci.*, **29**, 3743–8 (1994).

[30] I. Molodetsky, A. Navrotsky, M. J. Paskowitz, V. J. Leppert, and S. H. Risbud, "Energetics of X-ray Amorphous Zirconia and the Role of Surface Energy in its Formation," *J Non-cryst. Sol.*, **262**, 106–13 (2000).

[31] M. R. Ranade, S. H. Elder, and A. Navrotsky, "Energetics of Nanoarchitectured TiO_2–ZrO_2 and TiO_2–MoO_3 Composite Materials," *Chem. Mater.*, **14**, 1107–14 (2002).

[32] S. V. Ushakov, C. E. Brown, A. Navrotsky, A. Demkov, C. Wang, and B. -Y. Nguyen, "Thermal Analyses of Bulk Amorphous Oxides and Silicates of Zirconium and Hafnium," *Mater. Res. Soc. Symp. Proc.*, **745**, 3–8 (2003).

[33] I. -W. Chen and Y. -H. Chiao, "Martensitic Nucleation in ZrO_2," *Acta Metall.*, **31**, 1627–38 (1983).

[34] R. J. Wilson, "Calorimetry"; pp. 129–65 in *Principles of Thermal Analysis and Calorimetry*, Edited by P. J. Haines. The Royal Society of Chemistry, Cambridge, UK, 2002.

[35] F. D. Rossini, D. D. Wagman, W. H. Evans, S. Levine, and I. Jaffe, "Selected Values of Chemical Thermodynamic Properties," *Circ. Natl. Bur. Stand. (US)*, 500 (1952).

[36] R. A. Robie and B. S. Hemingway, "Thermodynamic Properties of Minerals and Related Substances at 298.15 K and 1 Bar (10^5 Pascals) Pressure and at Higher Temperatures," *U.S. Geol. Surv. Bull.*, 2131 (1995).

[37] W. M. Latimer, *Oxidation Potentials*, 2nd edition. Prentice-Hall Inc., New York, NY, 1952.

[38] A. G. Turnbull, "Thermochemistry of Zirconium Halides," *J. Phys. Chem*, **65** [9] 1652–4 (1961).

[39] S. R. Morrison, "Chemisorption on Nonmetallic Surfaces"; pp. 199–229 in *Catalysis Science and Technology*, Vol. 3. Edited by J. R. Anderson, and M. Boudart, Springer-Verlag, New York, 1982.

[40] J. P. Coughlin and E. G. King, "High-Temperature Heat Contents of Some Zirconia Containing Substances," *J. Am. Chem. Soc.*, **72**, 2262–5 (1950).

[41] T. Tojo, T. Atake, T. Mori, and H. Yamamura, "Excess Heat Capacity in Yttria Stabilized Zirconia," *J. Therm. Anal. Cal.*, **57**, 447–58 (1999).

[42] T. Tojo, T. Atake, T. Mori, and H. Yamamura, "Heat Capacity and Thermodynamic Functions of Zirconia and Yttria-stabilized Zirconia," *J. Chem. Thermodyn.*, **31**, 831–45 (1999).

[43] I. -W. Chen and Y. -H. Chiao, "Martensitic Nucleation in ZrO_2 and HfO_2—An Assessment of Small Particle Experiments with Metal and Ceramic Matrices";

pp. 33–45 in *Science and Technology of Zirconia II. Advances in Ceramics*, Vol. 12. Edited by N. Classen, M. Rühle, and A. H. Heuer. American Ceramic Society, Westerville, OH, 1984.

[44] I. -W. Chen and Y. -H. Chiao, ''Theory and Experiment of Martensitic Nucleation in ZrO_2-Containing Ceramics and Ferrous Alloys,'' *Acta. Metall.*, **33**, 1827–45 (1985).

[45] A. Christensen and E. A. Carter, ''First Principles Study of the Surfaces of Zirconia,'' *Phy. Rev. B*, **58** 12] 8050–64 (1998).

[46] W. D. Kingerey, ''Absolute Measurement of Metal–Ceramic Interfacial Energy and the Interfacial Adsorption of Silicon from Iron–Silicon Alloys''; in *Study of Metal–Ceramic Interactions at Elevated Temperatures*, Edited by F. H. Norton, W. D. Kingery, G. Economos, and M. Humenik. U.S. Atomic Energy Commission, NYO-3144, NSF, Washington, DC, 1953.

[47] L. Wang, K. Vu, A. Navrotsky, R. Stevens, B. F. Woodfield, and J. Boerio-Goates, ''Thermodynamics of CoO Nanoparticles,'' *Chem. Mater.* (in press).

□